

Kinetics, isotherm and thermodynamic studies on the adsorption of methylene blue dye by iron doped activated carbon

A. Revathi*, P. N. Palanisamy

Centre for Environmental Research, Department of Chemistry, Kongu Engineering College, Perundurai, Tamilnadu, India

The present study details the synthesis and characterisation of iron (Fe) doped activated carbon from *Alstonia Scholaris* (AS-Fe) natural wood waste. Investigation addresses the utilization of natural wood waste for useful and potential high temperature *Alstonia Scholaris* activated carbon (HT-AS). Iron doped activated carbon (AS-Fe) is used for the treatment of industrial waste water. Activated carbon and utilization performances are well attributed to the preparation methods and hence a range of characteristic interpretation like Fourier transform spectroscopy (FTIR), X-Ray powder diffraction, UV-Vis spectra, Field emission Scanning Electron Microscopes (FE-SEM) and EDAX analysis are evaluated. The result of AS-Fe is well distinguished by comparing the features with the porous high temperature *Alstonia Scholaris* activated carbon (HT-AS). High-performing iron doped activated carbon (AS-Fe) developed from natural wood waste reveals a distinct advantage in the adsorption approach for the removal of organics such as synthetic textile colours from industrial wastewater.

(Received January 10, 2022; Accepted April 1, 2022)

Keywords: Adsorption, *Alstonia scholaris*, Methylene blue, Wastewater, Iron doped

1. Introduction

In the present scenario, researchers dealing with adsorption techniques [1] show great interest in the search for low-cost, eco-friendly methods for the treatment of textile dyes [2] and inorganics in the industrial wastewater [3-5]. With the increasing industrialisation [6], the collection of wood wastes in the surroundings and their disposal faces a great challenge [7-8]. Hence, this research concentrates on handling one such waste from surroundings. Adsorption by activated carbon process is extensively used for eradicating organic dye pollutants from aqueous solution, and it has been verified to be an effective and consistent treatment for organic dyes. Activated Carbon is an important one by using renewable feedstock for biomass sources like agricultural waste, sewage sludge, wood waste etc., which has established large attention, not only for being cheap, renewable and existing in large quantities, but also forestry wastes and agricultural wastes are high carbon and low ash contents [9 -12]. *Alstonia Scholaris* wood and such materials are expected to be cost effective and environmentally beneficial, despite the fact that it is not utilised for any other purposes in any form. Preferably, *Alstonia Scholaris* wood activated carbon [7,13 -16] can also be made from low-cost agricultural waste [16-17], which is a successful inexpensive precursor [18-19]. Despite using this type of wood waste as a purposeful adsorbent, it can be utilized as viable remedy for discarding them into the environment. The improvisation and modification to a characterised adsorbent are the key aspects of the current research.

In current studies, the magnetically separable nano-sized adsorbent [20-21] attributed as an attractive area of research due to its remarkable magnetic properties [16, 17] and for its widespread application in the various fields [5,15]. The extensive application of such products also promoted their utilisation in the wastewater treatment processes [18 -20]. The performance of this type of adsorbent can be synthesised using methods like sonicate process, chemical activation co-precipitation etc. which is preferred for its effortlessness [22, 15]. Likewise, the introduction of

* Corresponding author: dhanukr10@gmail.com
<https://doi.org/10.15251/DJNB.2022.172.431>

such magnetic property [22] to the wood waste carbon also captures spotlight to overcome the hurdles in the wastewater treatment. The main aim of the present report is to bring up a simple way for achieving cost effective, structurally improved [23] and useful adsorbent [3]. The study also investigates the elevation in characteristics and textural properties of the iron doped precursor.

2. Materials and methods

2.1. Chemicals

Chemicals employed in all the experiments were of analytical grade (AR) and sourced from Global Scientific Chemicals, Erode. The Methylene blue dye was procured from Dystar India. The chemicals used in this study were Ferrous Sulphate, Ferrous Ammonium sulphate, Sulphuric Acid, Sodium hydroxide, Double distilled water and Methylene blue dye.

2.1.1. Synthesis of AS-Fe doped adsorbent

The collected *Alstonia Scholaris* wood waste from local area was dried, powdered and activated using concentrated sulphuric acid-maintained at atmosphere (> 500 °C) using muffle furnace. The powdered activated carbon (HT-AS) was taken and added 3:1:1 ratio of $\text{FeSO}_4 \cdot 7\text{H}_2\text{O}$ and FAS. At this point, freshly prepared sodium hydroxide was added dropwise to attain the pH level of 8-9. The resultant precipitate was sonicated, washed with double distilled water and then dried in a hot air oven at 100°C for 24 hours. The resultant powder was used as adsorbent. The prepared iron doped *Alstonia Scholaris* Activated carbon was named as AS-Fe.

2.1.2. Analysis methods of Adsorbent

The analytical techniques (BIS standard) were employed to represent the chemistry of the samples taken for study [24]. FTIR spectra of the samples were attempted on Fourier transform infrared spectrometer (IR Affinity-1) using KBr technique to verify the presence of functional groups. The diffraction peaks and phase transformation were studied on X-pert Pro-P Analytic using 40 kV, Cu $K\alpha$ radiation. The surface morphological analysis were carried out by FE-SEM and EDAX analysis was attempted to portray the structural formation of HT-AS and AS-Fe using Zeiss (voltage @ 30 KV). TG-DTA analysis was studied for the samples to better explore the thermal stability of the substance present.

3. Results and discussion

3.1. FE-SEM Analysis

Initially Fig. 1(a) pictures the appearance of HTAS with wide pores in it, However, the image of AS-Fe as in Fig. 1(b) shows highly porous like structures ensuring the high chance of adsorption with larger amount of adsorbate on it. The carbon and porous content are expected to be relatively higher than the precursor. This structure of HT-AS with active pores can be widely noted in Fig 1a. The precipitation of iron oxide nanoparticles onto the carbon structure is hence well figured in Fig. 1(b). This picture clearly depicts the existence of iron oxide nanoparticles into the surface of high temperature activated carbon.

The EDAX analysis is meant to confirm the accurate composition of the attempted samples. This analysis confirms the existence of high carbon in HT-AS (Fig. 2(a)). The results depicted, projects a clear understanding of the occurrence of iron oxide onto the high temperature activated carbon (Fig. 2(b)).

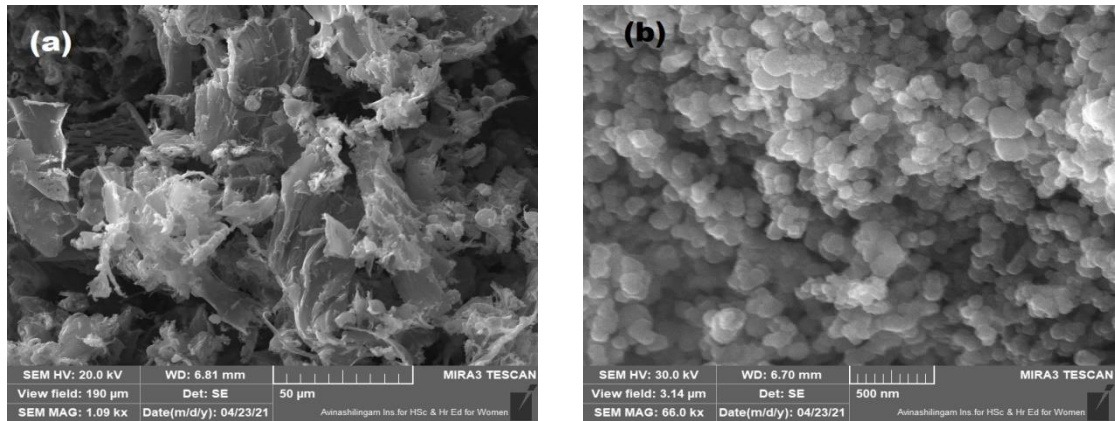


Fig. 1. FE-SEM image of (a) HT-AS and (b) AS-Fe.

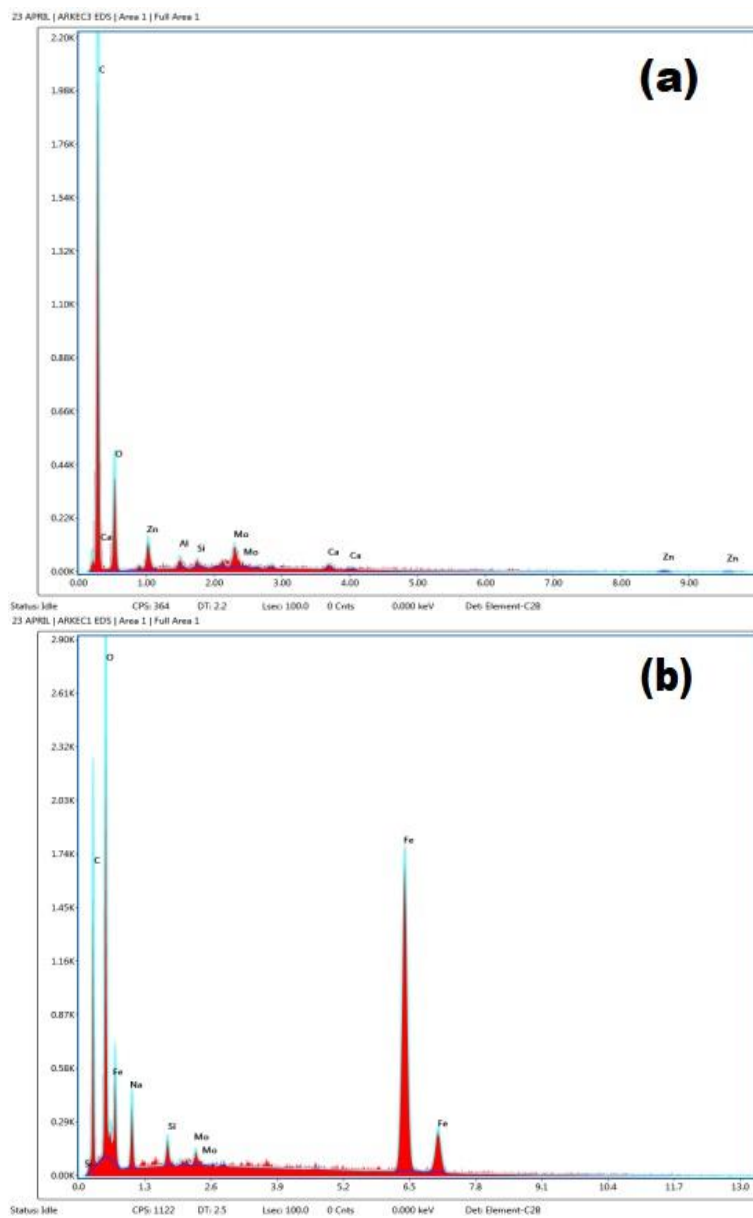


Fig. 2. EDAX analysis of (a) HT-AS and (b) AS-Fe.

3.2. XRD Analysis

The X-Ray diffraction (XRD) patterns elucidate the phase structure of HT-AS (Fig.3(a)) and AS-Fe (Fig. 3(b)). The broad clustered peaks indicate the amorphous nature of HT-AS and this may be due to the high-temperature activation. The high-intensity peak at $2\theta = 25^\circ$ signifies the presence of amorphous carbon in HT-AS [25]. The presence of iron component in AS-Fe composite is examined by portraying the sharp peaks and few clustered peaks in it. These sharp peaks indicate the presence of crystalline nature and few clustered peaks also confirm the existence of amorphous activated carbons [26]. The diffraction peaks at 2θ values of 33.53, 35.84, 36.87, 42.97, 48.98, 2.32, 59.20, 62.39° and relative intensity are considerably nearer to the standard data of rhombohedral haematite iron oxide lattice structures identified [27].

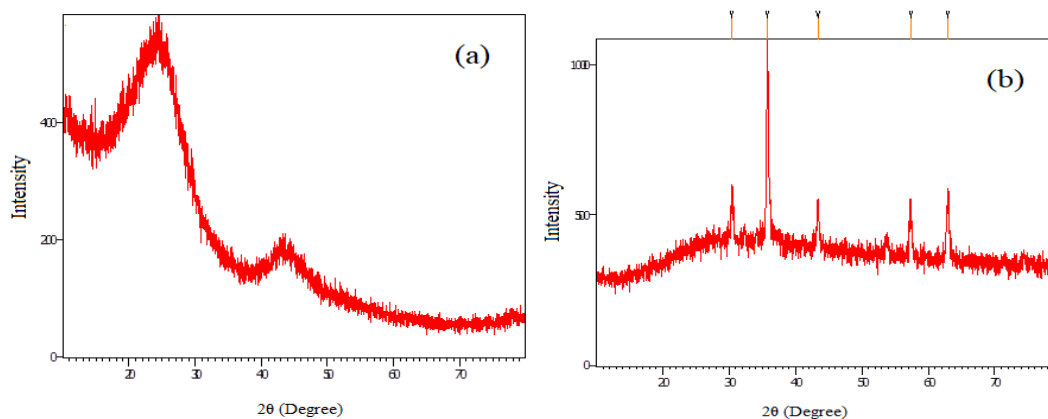


Fig. 3. XRD analysis of (a) HT-AS and (b) AS-Fe.

3.3. FTIR Analysis

The functional groups of the prepared samples are predictable from FTIR spectral study. Furthermore, it can consequently support in the interpretation of the functional groups Fig.4.

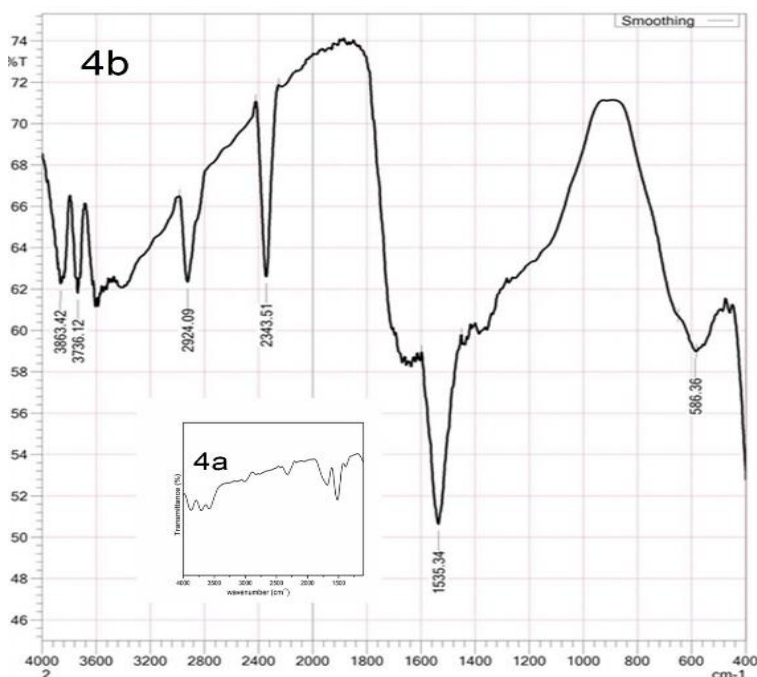


Fig. 4 FTIR Analysis (a) HS-AC and (b) AS-Fe.

The spectral image is given in Fig.4(a) and the absorption band of the precursor HT-AS and the modification in its structure to AS-Fe can be noted in Fig 4(b). The absorption bands around 3500 cm^{-1} for HT-AS and AS-Fe is attributed to intramolecular H-bonds [28]. The spectra of HT-AS and AS-Fe depict a considerable peak at 3736.12 cm^{-1} which may be due to the presence of H-bonded- OH stretch [28] that portrays the existence of hydroxyl group [18]. The troughs around 3900 cm^{-1} for HT-AS and AS-Fe (Fig.4(b)) are attributed to an aliphatic group (C-H) [29]. The existence of CH_3 shows a trough in the range of 1535 cm^{-1} in HT-AS and AS-Fe respectively. The new stretching peaks below 1535.34 cm^{-1} confirms the existence of iron oxides in [30] AS-Fe composite.

3.4. Batch Adsorption studies

It is essential to optimise the reaction mechanism between the prepared HT-AS and AS-Fe in the removal of methylene blue using batch adsorption characteristics such as optimum pH, optimum agitation time and initial concentration. These reactions are carried out at room temperature. Both the samples are attempted in the removal of methylene blue at various initial concentrations, agitation time and pH. The results in the uptake of methylene blue from water by AS-Fe increases from 77 to 100% when the agitation time was varied from 10 to 100 minutes and attains equilibrium in 60 minutes at 273 K and at pH 7.0. Meanwhile, the initial concentration of the methylene blue solution used was 20 ppm and the adsorbent dosage was 300 mg. The increase in adsorption of methylene blue with increase in agitation time may be accredited to the increased intra particle diffusion taking place during long shaking time. The initial concentration of methylene blue dye solution was varied (20, 40, 60, 80 and 100 ppm) and batch adsorption experiments were supported with 300 mg of the adsorbent at 273 K and at $\text{pH} \approx 7.0$. An increase in the removal percentage of methylene blue from 72 to 92.5% observed with 300 mg of the adsorbent in agitation time of 60 minutes when the initial concentration of the methylene blue solution was varied at 20, 40, 60, 80 and 100 ppm. The higher uptake of methylene blue at low concentration may be attributed to the more availability of active center on the surface of the adsorbent for lesser number of adsorbate species. Methylene blue adsorption curves are smooth, single and continuous signifying the possible monolayer coverage of dye molecules on the surface of the adsorbent.

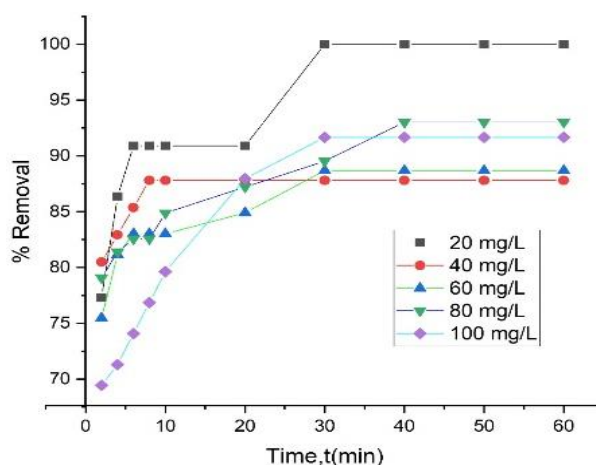


Fig. 5 Effect of Agitation Time on dye removal

3.5. Isotherm Adsorption Studies

The isotherm studies are essential in assessing the adsorption efficiency of the adsorbent. Several isotherm models are practised in describing the adsorption technique, among them essential isotherm models such as Langmuir (Fig.6(a)) and Freundlich isotherm (Fig.6 (b)) models are utilised in this study for the analysis of adsorption of methylene blue. In this respect, the Langmuir isotherm is more essential, though the restrictions and the limitations of this model have

been well recognised. The Langmuir and the rearranged Langmuir equations (Equation (1) and (2)) are given

$$1/q_e = 1/Q_0 b \cdot 1/C_e + 1/Q_0 \quad (1)$$

$$C_e/q_e = C_e/Q_0 + 1/Q_0 b \quad (2)$$

From the slope value, the suitability of Langmuir monolayer adsorption model is noted to be favourable. The results of the model apply to the better fit of monolayer Langmuir. The R^2 values from the plot $\log q_e$ vs $\log C_e$ represents the favourable Freundlich model. R_L value is one of the prime characteristics of Langmuir patterns. The results are tabulated in Table 1. From the results, it is well-known that both adsorbents are not favourable for monolayer pattern. Further, the separation factor of R_f value resulted are mentioned in the below Table 1 denote a favourable process of adsorption between the prepared AS-Fe adsorbents and dye molecules.

The linear form of Freundlich Equation (3) is represented as

$$\log x/m = \log k_f + 1/n \log C_e \quad (3)$$

where, 'x' is the amount of methylene blue adsorbed in mg. 'm' is the weight of adsorbent (g) C_e is the residual concentration of methylene blue at equilibrium in mg. k_f and $1/n$ are Freundlich constants related to the adsorption capacity and adsorption intensity respectively and are evaluated by least square fitting of the data by plotting $\log x/m$ vs $\log C_e$ with a slope of $1/n$ and intercept of $\log K_f$

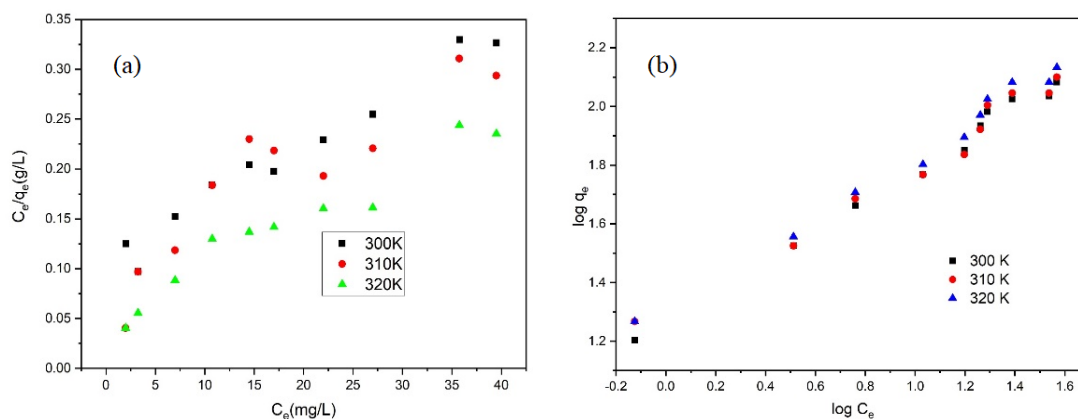


Fig. 6. (a) Langmuir isotherm and (b) Freundlich isotherm.

The Freundlich adsorption isotherm has been obtained in 60 minutes of agitation time. The values of $R_f > 1$, obtained in this study indicates the applicability of Langmuir adsorption isotherm. The R^2 value varied at 0.99 at 300K and 0.98 at 310K temperature. The obtained isotherm linear regression values (R^2) were closer to unity which formerly indicates the adsorption of methylene blue on AC-Fe that follow the Freundlich isotherm model than Langmuir isotherm model. From the pseudo second order plot values of adsorption intensity $1/n \gg 1$ reveals the applicability of this adsorption isotherm. The values of K_L are given in the Table 1. The study of temperature effects on the Freundlich parameters reveals that an increasing trend in the adsorption capacity with temperature. The correlation coefficient values obtained for Freundlich isotherm model convey the favourable activity by adsorbents in the reaction mechanism towards methylene blue dye solution. Therefore, on comparing the two isotherm models, the adsorption mechanism in this work was well analysed and their results conclude that the AS-Fe is a capable adsorbent in the removal of synthetic dye molecules from the aqueous solutions.

Table 1. Parameters of Langmuir and Freundlich Adsorption Isotherms for MB onto AS-Fe.

Temperature (K)	Langmuir Isotherm			Freundlich Isotherm		
	K_L (L mg ⁻¹)	R_L	R^2	1/n	K_f (mg g ⁻¹)	R^2
300	0.06	0.02	0.96	0.52	18.29	0.99
310	0.08	0.02	0.88	0.50	19.93	0.98
320	0.11	0.02	0.92	0.52	20.46	0.99

3.6. Kinetic Adsorption Studies

In order to examine the mechanism of sorption and potential monitoring steps such as mass transport, a few kinetic models were confirmed with the pseudo first order kinetic model, the Elovich model and the pseudo second order kinetic model as indicated in equation (4), (5) and (6) (Fig. 7(a), (b) and (c)). For a batch contact time process, where the rate of sorption of dye to the specified adsorbent is proportional to the amount of dye sorbed from the solution phase [31].

PSEUDO FIRST ORDER KINETIC MODEL

$$\log (q_e - q_t) = \log q_e - k_{\text{lager}} 2.303 * t \quad (4)$$

ELOVICH MODEL

$$q_t = \beta \ln(\alpha \beta) + \beta \ln t \quad (5)$$

PSEUDO SECOND ORDER KINETIC MODEL

$$dq_e / dt = k_2 (q_e - q_t)^2 \quad (6)$$

This study on kinetics gives the interaction time between the adsorbate and adsorbent. This adsorption studies results in the rate and its value indicating the successful adsorption of methylene blue (Table 2). The experimental value was not encouraging to the calculated R^2 and q_e value and hence the adsorption process does not suit the pseudo-first order model. The pseudo-second order kinetic pattern was developed and the plot ($\frac{t}{q_e}$ Vs t) was mapped. The dye adsorption capacity (q_e) with the initial concentration of 10 mg/L with varying time intervals was 63 - 131 mg/g. The correlation coefficient for the pseudo-second order model ($R^2 = 0.999$) was almost equal to unity denoting the better inference of the process between AS-Fe which can be utilized for the adsorption of methylene blue. These plots show the data fits had good correlation coefficients (> 0.997) when the pseudo second order equation was employed; it was possible to ascertain from them whether the rate determining process is a chemical reaction or not [32]. Thus, increasing the initial dye concentration from 20 mg/L to 100mg/L the methylene blue adsorbed at any contact time increases. This is understandable for higher initial concentration values, as a more efficient utilization of the sorptive capacities of the sorbent would be projected due to greater sorption driving force.

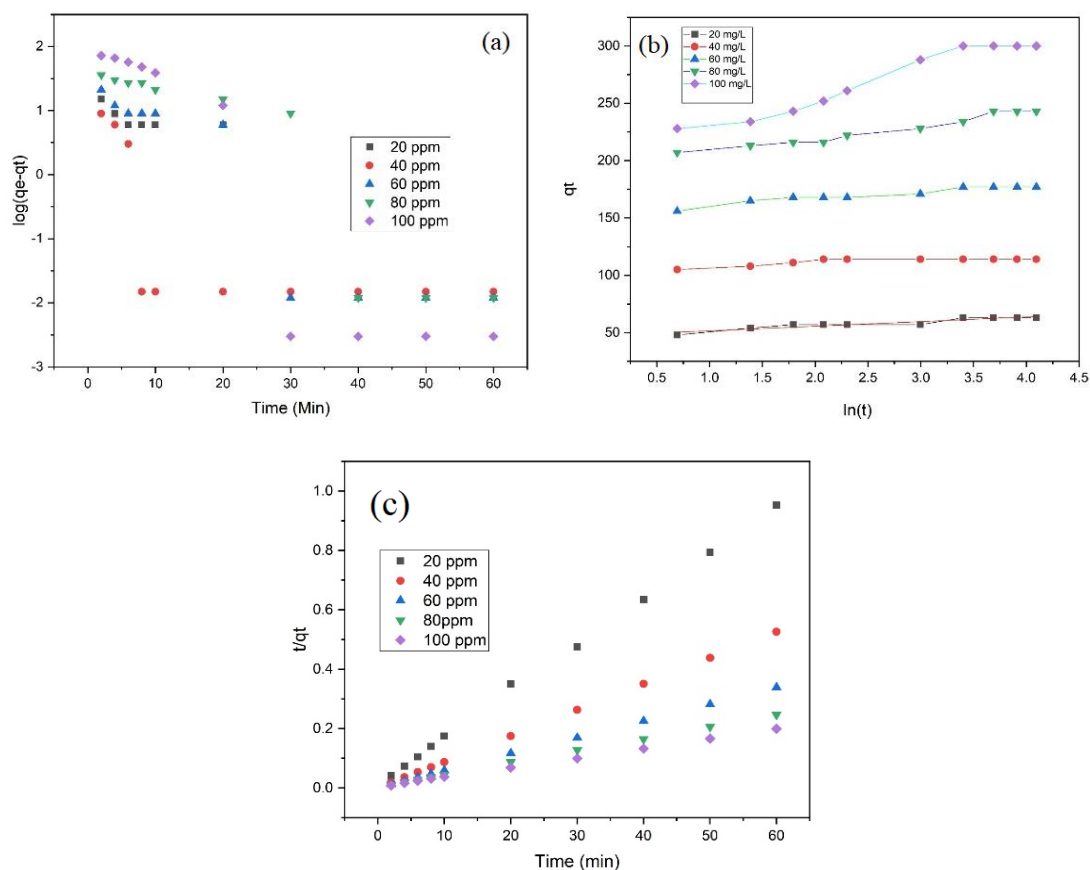


Fig. 7. Kinetic Adsorption Studies (a) Pseudo first order kinetic model, (b) Elovich Model and (c) pseudo Second order kinetic model.

3.7. Adsorption Thermodynamics

Thermodynamic pattern describes the reaction process in a nominal way. In this present work, thermodynamic pattern was evaluated along with their macroscopic parameters such as a change in enthalpy, change in entropy, and free energy (Equation (7) and (8)). These constants were determined at three different temperatures (300, 310 and 320 K). The calculations were made by the equations followed by [21]

$$\Delta G = - RT \ln K \quad (7)$$

$$\Delta S = (\Delta H - \Delta G)/T \quad (8)$$

The results are calculated accordingly, such that the positive values of entropy (ΔS), enthalpy (ΔH) for the adsorbents and portray their endothermic nature Fig.8. The negative free energy (ΔG) indicates the processes exhibited are spontaneous and feasible in nature (Table.3). This provides the quantitative adsorption process of AS-Fe with the dye molecules.

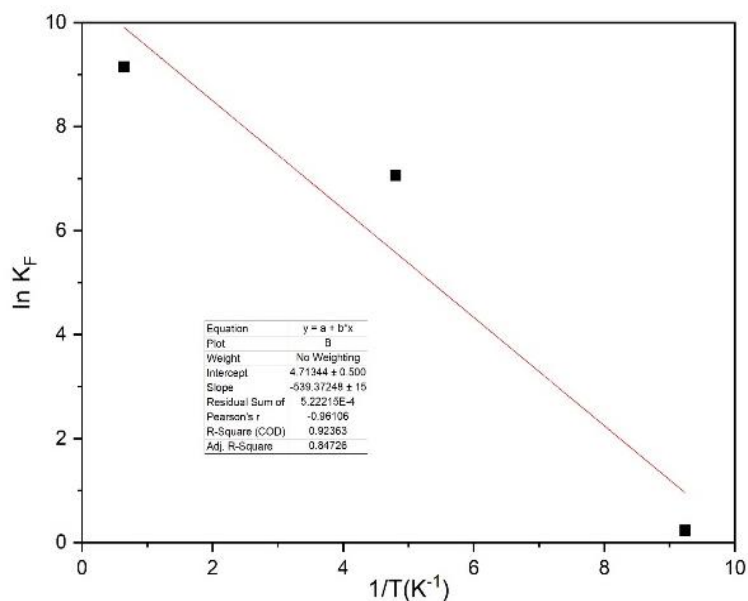


Fig. 8. A Plot of $1/T$ Vs $\log K_F$.

Table 2. Kinetic Model Values for the Adsorption of MB on to AS-Fe.

Conc. (mg/L)	Pseudo First Order Values				Elovich Values			Pseudo Second Order Values		
	qe,exp (mg/g)	k1 (min-1)	qe,cal (mg/g)	R ²	α	β	r ²	k1 (min-1)	qe,cal (mg/g)	R ²
20	63	0.04	10	0.24	48	4.0	0.88	0.02	64	0.99
40	114	0.09	1	0.32	106	2.3	0.63	0.07	114	0.99
60	177	0.15	24	0.83	106	2.3	0.63	0.01	179	0.99
80	243	0.16	94	0.84	155	5.7	0.92	0.00	246	0.99
100	300	0.22	145	0.84	196	11.6	0.96	0.00	308	0.99

Table 3. Thermodynamic Parameters for the Adsorption of MB on AS-Fe

Temperature (K)	ΔG^0 (kJmol ⁻¹)	ΔH^0 (kJ mol ⁻¹)	ΔS^0 (J mol ⁻¹ K)
300	-7.25	4.484	39.19
310	-7.46		
320	-7.53		

4. Conclusion

The performance of AS-Fe in the adsorption process for the removal of methylene blue are investigated in this study using an agricultural wood waste, *Alstonia Schloris* was evaluated as an eligible activated carbon (HT-AS) in the adsorption process and the iron-oxide doped activated carbon (AS-Fe) was synthesised and Fourier-transform Infrared spectroscopy (FTIR) resulted with

the ranges proving the presence of the adsorbed dye molecules in the adsorbent. The isotherm study was carried out at the optimised pH, dose and at temperatures ranging from 300 K – 320 K equilibrated for sixty minutes which postulated the Freundlich isotherm adsorption and the maximum Q_m (mg/g) was 136 mg/g for AS-Fe – methylene blue. The isotherm studies Langmuir and Freundlich type of isotherm equations and their results support the monolayer type of adsorption between dye molecules and adsorbents. The correlation coefficient R^2 value was 0.999 resulted in the best fitted pseudo-second order kinetics. The positive enthalpy (ΔH) results in the endothermic nature involved and negative values of ΔG project the feasibility and spontaneity of the adsorption reaction. The AS-Fe improved its potential in the removal of methylene dye and found to be enhanced and effective in the adsorption of basic dyes adopting the constructive analytical technique.

References

1. S. Sophie Beulah, K Muthukumar, E-J of Chem, 7(1), 299-307(2010); <https://doi.org/10.1155/2010/928248>
2. G. Moussavi, & M. Mahmoudi, Journal of hazardous materials, 168(2-3), 806-812, (2009); <https://doi.org/10.1016/j.jhazmat.2009.02.097>
3. R. A. Reza, M. Ahmaruzzaman, Rsc Advances, 5(14), 10575-10586; <https://doi.org/10.1039/C4RA13601B>
4. A. Et, S. Shahmohammadi-Kalalagh, Caspian Journal of Environmental Sciences, 9(2), 243-255 (2011).
5. F. M. Machado, C. P. Bergmann, T. H. Fernandes, E. C. Lima, B. Royer, T. Calvete & S. B. Fagan, Journal of hazardous materials, 192(3), 1122-1131(2011); <https://doi.org/10.1016/j.jhazmat.2011.06.020>
6. S. Chowdhury, M. Mishra, O.M. Suganya, Ain Shams Engineering Journal, 6(2), 429-437(2015); <https://doi.org/10.1016/j.asej.2014.11.005>
7. S. Nirmaladevi, P.N. Palanisamy, Cellulose Chemistry and Technology, 53(9-10), 1029-1039(2019); <https://doi.org/10.35812/CelluloseChemTechnol.2019.53.101>
8. K. Yang, J. Peng, C. Srinivasakannan, L. Zhang, H. Xia, X. Duan, Bioresource technology, 101(15), 6163-6169 (2010); <https://doi.org/10.1016/j.biortech.2010.03.001>
9. V. Senthil Kumar, A. Revathi, R. Priyadharsini, NP. Sasikumar, R. Senjudarvannan, D. Sudha, International Journal of Interdisciplinary Global Studies 130-134(2020).
10. I.K. Erabee, A. Ahsan, A.W. Zularisam, S. Idrus, N. N. N. Daud, T. Arunkumar, R. Sathyamurthy, E. Al -Rawajfeh, , Engineering Journal, 21 (2017) 1; <https://doi.org/10.4186/ej.2017.21.5.1>
11. A.M. Herrera -Gonzalez, M. Caldera -Villalobos, A.A. Pelaez -Cid, Journal of Environmental Management, 234, 237(2019); <https://doi.org/10.1016/j.jenvman.2019.01.012>
12. M.J. Sweetman, D. Sebben, B. D. Noll, W.H. Wang, Water Supply, 18, 371(2018); <https://doi.org/10.2166/ws.2017.123>
13. A. Revathi, A. Geetha, M. Asaithambi, P.N. Palanisamy, International Journal of Advance Research in Science & Engineering, 3, 11-23(2014).
14. S. N. F. Ali, E.I. El -Shafey, S. A l -Busafi, A.J. Al -Lawati, Journal of Environmental Chemical Engineering, 7 (2019) 1
15. S. N. Ali, E. I. El-Shafey, S. Al-Busafi, H. A. Al-Lawati, Journal of environmental chemical engineering, 7(1), 102860(2019); <https://doi.org/10.1016/j.jece.2018.102860>
16. F. Kanwal, R. Rehman, I. Q. Bakhsh, Journal of Cleaner Production, 196, 350-357(2018); <https://doi.org/10.1016/j.jclepro.2018.06.056>
17. J.C. Xu, P.H. Xin, Y. B Han, P.F. Wang, H.X Jin, D.F. Jin, X.L. Peng, B. Hong, J. Li , H.L. Ge, Z.W. Zhu, X.Q. Wang, J of Alloys and Compounds, 617, 622-626(2014); <https://doi.org/10.1016/j.jallcom.2014.08.059>

18. T. G. Yan, L. J. Wang, *Water science and technology*, 69(3), 612-621(2014); <https://doi.org/10.2166/wst.2013.745>
19. H. Y Zhu, Y. Q Fu, R. Jiang, J.H. Jiang, L. Xiao, G.M. Zeng, G. M & y. Wang, *Chemical Engineering Journal*, 173(2), 494-502(2011); <https://doi.org/10.1016/j.cej.2011.08.020>
20. S. Indhu, K. Muthukumar, *Digest Journal of Nanomaterials and Biostructures* 13(1), 201 - 213(2018).
21. R. Sudha, K. Srinivasan, P.Premkumar, *Eco. And Environ. Safety* 117,115-123(2015); <https://doi.org/10.1016/j.ecoenv.2015.03.025>
22. S. Indhu, K. Muthukumar, *Journal of Environmental Chemical Engineering*, 6(2), 3111-3121(2018); <https://doi.org/10.1016/j.jece.2018.04.027>
23. W. Ngarmkam, C. Sirisathitkul, C. Phalakornkule, *Journal of environmental management*, 92(3), 472-479(2011); <https://doi.org/10.1016/j.jenvman.2010.08.031>
24. A.O. Dada, A.P.Olalekan, A.M. Olatunya, O. Dada, *J of Applied Chem*,1(3) 2278-5736,38-45 (2012).
25. J. H. Kwon, L. D. Wilson,R. Sammynaiken, *Synthetic metals*, 197, 8-17(2014); <https://doi.org/10.1016/j.synthmet.2014.08.010>
26. M.S. Shamsuddin., N.R.N. Yusoff, and M.A. Sulaiman, *Procedia Chemistry* (19) 558-565(2016); <https://doi.org/10.1016/j.proche.2016.03.053>
27. A.J. Rettie,,W.D. Chemelewski, B.R. Wygant, J. Lindemuth, J.F. Lin, D. Eisenberg, C.B. Mullins, *Journal of Materials Chemistry C*, 4(3), 559-567(2016); <https://doi.org/10.1039/C5TC03368C>
28. S. Nirmaladevi, P.N. Palanisamy, *Desalination and Water Treatment*, 175, 282-292(2020); <https://doi.org/10.5004/dwt.2020.24906>
29. K. G. Raj, & P.A.Joy, P. A, *Journal of environmental chemical engineering*, 3(3), 2068-2075(2015); <https://doi.org/10.1016/j.jece.2015.04.028>
30. H. Yang, Q. Feng, *Journal of hazardous Materials*, 180(1-3), 106-114 (2010); <https://doi.org/10.1016/j.jhazmat.2010.03.116>
31. S. Karthikeyan,B. Sivakumar, N. Sivakumar, *E-Journal of Chemistry*, 7(S1), S175-S184 (2010); <https://doi.org/10.1155/2010/138684>
32. M. Sujatha, A. Geetha, P. Sivakumar, P.N Palanisamy, *E-Journal of Chemistry*, 5(4), 742-753(2008); <https://doi.org/10.1155/2008/418267>